Cardiovascular magnetic resonance imaging techniques in hypertension and diabetes

Brandts, A.

Anne Brandts
Matthias Stuber
Saskia G.C. van Elderen
Lucia J.M. Kroft
Stijntje D. Roes
Jouke T. Tamsma
Rob J. van der Geest
Hildo J. Lamb
Joost Doornbos
Hein Putter
Albert de Roos
Jos J.M. Westenberg

Chapter 03

Associations between Vessel Wall Thickness in the Aorta and Carotid Arteries and Aortic Pulse Wave Velocity in Patients with Hypertension: Assessment with MRI

Submitted

Abstract

Purpose

To evaluate the association between aortic pulse wave velocity (PWV) and aortic and carotid vessel wall thickness (VWT) using magnetic resonance imaging (MRI) in hypertensive patients as compared to healthy volunteers.

Materials and Methods

Local medical ethics approval was obtained and participants gave informed consent. Fifteen hypertension patients (5 men, 10 female, overall mean age 49 ± 14 years) and fifteen age- and sex-matched healthy volunteers were included. Aortic PWV and aortic and carotid artery VWT were assessed using validated MRI techniques. The paired t-test, Pearson correlation (r), uni- and multivariable stepwise linear regression analyses were used for statistical analyses.

Results

Mean values for aortic PWV and aortic and carotid artery VWT were significantly higher in hypertension patients as compared to healthy volunteers (aortic PWV 7.0 ± 1.4 m/s vs. 5.7 ± 1.3 m/s, aortic VWT 0.12 ± 0.03 ml vs. 0.10 ± 0.03 ml, carotid VWT 0.04 ± 0.01 ml vs. 0.03 ± 0.01 ml, all $p < 0.015$). Aortic PWV was significantly associated with aortic VWT (r 0.76 vs. 0.63) and to a lesser extent with carotid artery VWT (r 0.50 vs. 0.40) both in patients and controls. In addition, aortic VWT was associated with carotid VWT, both in patients and controls (r 0.60 vs. 0.57).

Conclusion

Using MRI, aortic PWV is significantly associated with aortic VWT and to a lesser extent with carotid VWT. These findings indicate the systemic nature of early vessel wall thickening associated with hypertension, potentially allowing for improved risk stratification of hypertensive vascular disease.

Introduction

Hypertension is an important public health concern leading to increased cardiovascular morbidity and mortality (1,2). An important prognostic factor in hypertension is arterial stiffening. Two possible mechanisms may explain this structural vascular stiffening: 1. arterial wall stretching due to distension; 2. structural arterial wall changes including wall thickening (3,4). However, the degree to which structural arterial wall changes account for hypertension-associated stiffening is still disputed (4).

Furthermore, these structural arterial wall changes are usually not confined to a localized arterial segment, but rather occur as a systemic disease (5). Previous studies revealed that arterial stiffness is associated with increased carotid wall thickness (i.e. intima-media thickness) and with the presence of carotid and aortic plaques in elderly and in hypertensive patients (6-8).

Magnetic resonance imaging (MRI) is a validated and accurate imaging technique to assess pulse wave velocity (PWV) and vessel wall thickness (VWT) (9-11). A previous MRI study has demonstrated an association between aortic VWT and aortic distensibility (as a measure of local aortic stiffness) (12). However, possible systemic nature of disease by comprehensive evaluation of both the aorta and carotid artery has not been established yet. Such evaluation would be desirable as to verify the conceivable systematic character of disease and to determine the relationship between morphological VWT and functional PWV parameters that may represent disease.

Accordingly, the purpose of this study was to evaluate the association between aortic PWV and aortic and carotid VWT using MRI in hypertensive patients as compared to healthy adult volunteers.

Materials and Methods

Study population

Approval from the local medical ethics committee was obtained and all subjects gave informed consent. Fifteen patients (5 men, 10 women, age range: 24-72 years, overall mean age 49 ± 14 years) diagnosed with essential hypertension defined as systolic blood pressure > 140 mmHg and/or diastolic blood pressure > 90 mmHg on repeated physical examination, before antihypertensive medication was instituted (2), were prospectively and consecutively included between March 2009 and October 2009. Exclusion criteria comprised of evidence of aortic valve stenosis or insufficiency, as evaluated by means of physical examination and velocity-encoded MRI, Marfan syndrome, aortic coarctation or any aortic disease, known history of systemic diseases other than hypertension and general contraindications to MRI. All patients were on treatment with antihypertensive medication at time of MRI.

Fifteen age-matched (within 2 years for each participant) and sex-matched healthy volunteers without history of cardiovascular disease were included for comparison. Healthy volunteers were recruited by advertisement and underwent a similar and previously described work-up as hypertensive patients (13). Blood pressure was measured at time of MRI using a semi-automated sphygmomanometer (Dinamap, Critikon, Tampa, Florida, USA). Furthermore, smoking status (i.e. non-smoker or current smoker or former smoker), body mass index (BMI), body surface area (BSA), the cholesterol to high-density lipoprotein (Cholesterol/HDL) ratio and C-reactive protein were determined. Blood was drawn in the morning after an overnight fast within two weeks of MRI. The albumin excretion ratio was calculated using the microalbumin and creatinin concentrations in the urine.

Pulse wave velocity

PWV was determined using a 1.5 T MRI scanner (Philips Intera, Philips Medical Systems, Best, the Netherlands) as described earlier (13). In short, on a scout image of the aorta (Figure 1a), a velocity-encoded (VE) MRI-sequence was planned perpendicular to the ascending and proximal descending aorta to assess the blood flow velocity. Scan parameters were: repetition time (TR) 5.0 ms, echo time (TE) 2.9 ms, flip angle (FA) 20°, field-of-view (FOV) 300 mm, 128 × 115 acquisition matrix, reconstructed to 256 × 256, slice thickness 8 mm with maximal number of phases reconstructed. The maximum velocity encoding (Venc) was set to 150 cm/s.

PWV was calculated by using the formula: $\Delta x/\Delta t$ (m/s), where Δx describes the distance along the aortic centerline between measurement sites in the ascending and the proximal descending aorta and Δt describes the transit-time of the arrival of the systolic pulse wave at these respective sites. The aortic path length between the ascending and proximal descending measurements sites was determined from a centerline manually positioned along the aorta (Figure 1a) using the previously validated in-house developed software package MASS (14). Transit-time was analyzed from aortic flow velocity maps (Figure 1b) using the previously validated in-house developed software package FLOW (14).

Semi-automatic contour drawing in the aorta velocity maps was performed by two researchers (A.A., with 3 years of experience in cardiac MRI) and supervised by a senior researcher (B.B. 16 years experience in cardiac MRI), both blinded to the subjects' condition.

Aortic vessel wall thickness

The aortic vessel wall MRI sequence was performed as described in the literature using a previously validated technique on a 3T MRI scanner (Achieva, Philips, Best, the Netherlands) (10). In short, a 3-dimensional dual-inversion black-blood , segmented *k*-space gradient-echo imaging sequence with fat suppression was localized perpendicular to the aorta at the level of the margin between the 8th thoracic vertebra and the intervertebral disc between the 7th and 8th vertebrae, to assess a 2-cm-thick 3-dimensional volume of the aorta (Figure 1c) (15).

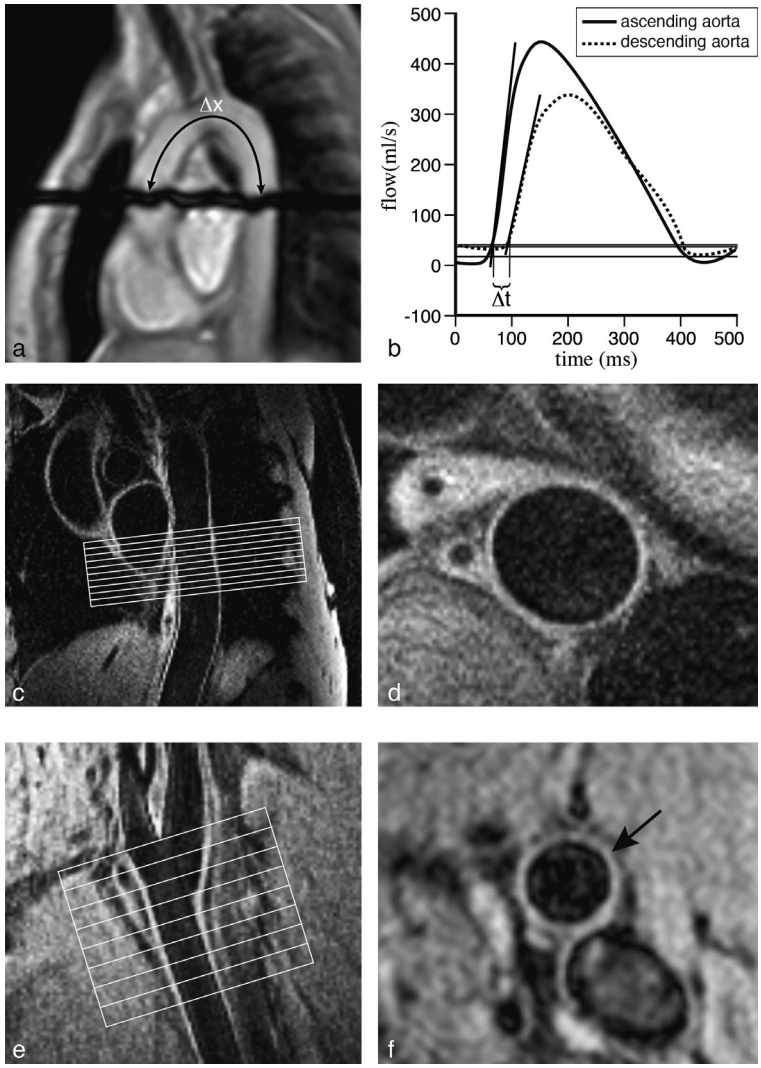

Figure 1. Scan protocol for assessment of aortic PWV and aortic VWT and left carotid VWT.

On a longitudinal scout image of the aorta (a), a velocity-encoded (VE) MRI-sequence was planned perpendicular to the ascending and proximal descending aorta (indicated by the black line) at the level of the pulmonary trunk, to assess the blood flow velocity in the ascending and proximal descending aorta. Δx represents the path length of the aorta along the centerline of the aortic arch. 1b represents the resulting flow curves measured at the two respective sites (in the ascending and descending aorta, respectively). The onset of the systolic wave front was automatically determined from this flow graph by detecting the intersection point of the horizontal line modeling the constant diastolic flow and upslope of the systolic wave front, modeled by linear regression along 20% to 80% of the range of the flow values along the upslope. Δt represents the transit time of the flow wave to propagate from the ascending to the descending aorta.

1c represents a double-oblique sagittal black-blood image with a 2-cm-thick 3-dimensional volume acquisition of the aorta vessel wall positioned perpendicular to the aorta at the level of the margin between the 8th thoracic vertebra and the intervertebral disc. 1d represents a resulting cross-sectional view of aorta and aortic vessel wall.

1e represents an oblique coronal black-blood image of the left carotid artery with a 1.6-cm-thick multi-slice 2-dimensional acquisition stack positioned perpendicular to the common carotid artery starting at the level of the carotid bifurcation (e). 1f represents a resulting cross-sectional view of the left carotid artery (arrow) and carotid vessel wall.

Scan parameters included: TR 4.9 ms, TE 2.5 ms, FA 20°, FOV 367 × 512 mm^2, scan matrix 512, acquired in-plane resolution 0.53 × 0.55 mm^2, reconstructed in-plane resolution 0.53 × 0.53 mm^2, slice thickness 2 mm, and NSA 2. Furthermore, data were acquired every other heartbeat to minimize the likelihood of slow blood flow contributing to artifactual enhancement at the periphery of the vessel lumen. Ten cross-sectional slices of the aorta of 2 mm thickness were reconstructed for further analysis.

Aortic vessel wall image analysis was performed using the previously validated in-house developed software package VesselMass (16). The aortic luminal and outer wall boundaries were detected using a semiautomated contour detection tool as has been described previously (Figure 1d) (16). The aortic center was localized manually per interactive mouse-click in each slice and automatically detected contours were manually adapted in regions where segmentation of the vessel wall was not considered adequate. In all subjects, contour segmentation was performed in at least eight out of ten slices. The mean VWT is represented by cross-sectional vessel wall area × slice thickness averaged over all included slices and is indexed for BSA and expressed in ml.

Aortic vessel wall contour segmentation was performed by two researchers (A.A., with 3 years of experience in cardiac MRI) and supervised by a senior researcher (B.B. 16 years experience in cardiac MRI), both unaware of the subjects' conditions.

Carotid vessel wall thickness

In all subjects the left carotid artery was examined using a 3T MRI scanner (Achieva, Philips, Best, the Netherlands). The carotid vessel wall sequence has been described and validated previously (9). In short, a standardized series of oblique axial slices were planned perpendicular to the course of the common carotid artery (Figure 1e). A total of eight contiguous transverse slices with 2-mm thickness were acquired for the analysis starting from the left carotid bifurcation in the proximal (caudal) direction. The left carotid bifurcation on the oblique sagittal scouts was used as a landmark to ensure that the acquisition was planned at the same location for all subjects. A multislice 2-dimensional stack with dual inversion recovery black-blood (DIR) (15), spoiled segmented *k*-space fast gradient-echo sequence with spectrally selective fat suppression was used to maximize contrast between the carotid wall and the lumen blood pool. Images were acquired at each RR interval. Scan parameters were: TR 12 ms, TE 3.6 ms, FA 20°, FOV 367 × 512 mm^2, scan matrix 512, acquired in-plane resolution 0.82 × 0.86 mm^2, reconstructed in-plane resolution 0.82 × 0.82 mm^2, slice thickness 2 mm, and NSA 1.

Carotid vessel wall image analyses were performed using the previously validated in-house developed software package VesselMass in a similar way as described for the aortic vessel wall (Figure 1f) (16,17). In all subjects, contour segmentation was performed in at least four slices out of eight.

Carotid vessel wall contour drawing was performed by two researchers (A.A., with 3 years of experience in cardiac MRI) and supervised by a senior researcher (B.B. 16 years experience in cardiac MRI), both blinded to the subjects' conditions.

Statistical Analyses

Statistical analysis was performed using SPSS for Windows (version 17.0; SPSS, Chicago, Illinois, USA). Data are expressed as mean ± standard deviations (sd) unless stated otherwise. The paired sample t-test was used to compare the clinical, laboratory and MRI derived parameters between the age- and sex-matched hypertensive patients and healthy volunteers. Univariable linear regression analyses were performed in volunteers and hypertensive patients separately. First, the associations for aortic PWV, aortic VWT and carotid VWT with age were examined. Then the associations for aorta and carotid wall thickness with aortic PWV were examined. Furthermore, the association between aorta and carotid wall thickness was examined.

To test whether the regression coefficients were different between volunteers and hypertensive patients, multiple linear regression was performed with aortic PWV as dependent variable and hypertension status (i.e. no/yes; no=healthy volunteer) and the interaction between hypertension status with aortic PWV as predictors. A significant interaction indicates significantly different regression lines between volunteers and hypertensive patients. Slope ± standard error (se), intercept ± se and Pearson's correlation coefficients (r) are reported. A p-value of < 0.05 is considered statistically significant.

Results

Table 1 describes the clinical, laboratory and MRI derived parameters of hypertensive patients and healthy volunteers. As expected, hypertensive patients had higher systolic blood pressure than healthy volunteers ($p < 0.001$). BSA was similar between both groups. PWV was statistically significantly higher in hypertensive patients when compared to the matched controls ($p = 0.011$). Furthermore, the values for aortic VWT, aortic diameter and carotid VWT were significantly higher in hypertensive patients than in controls (i.e. $p < 0.001$, $p = 0.039$ and $p = 0.025$, respectively). These findings remained after indexing for BSA, except for aortic diameter which was no longer significantly different between patients and healthy adult volunteers. Therefore, aortic diameter was not included in subsequent analyses.

The associations between age, aortic PWV and VWT in the aorta and carotid arteries are presented in Figure 2. In Table 2, the results for the univariable regression analyses and correlation coefficients, indicating the strengths of the associations of the respective parameters, are presented. Both in patients and in volunteers, PWV was significantly associated with age, with Pearson $r = 0.74$ in hypertensive patients and $r = 0.70$ in volunteers. The association

Table 1. Comparison of hypertensive patients with age- and sex-matched healthy volunteers.

	Hypertension	*Volunteers*	*p-value*
Male/Female	5/10	5/10	0.10
Age	49 ± 14	49 ± 14	0.36
Smoking			
No/yes/former	11/3/1	10/1/4	0.24
Systolic blood pressure (mmHg)	149 ± 19	124 ± 12	<0.001*
Diastolic blood pressure (mmHg)	88 ± 13	80 ± 8	0.07
BMI (kg/m2)	26.9 ± 4.6	25.1 ± 3.3	0.24
BSA (m^2)	1.9 ± 0.2	1.9 ± 0.2	0.98
Cholesterol/HDL ratio (mmol/l)	3.4 ± 0.9	3.5 ± 1.2	0.78
C-reactive protein	6.5 ± 11.6	2.1 ± 3.5	0.16
Microalbuminuria/creatinine ratio	1.8 ± 2.0	23.6 ± 83.3	0.36
Aortic PWV (m/s)	7.0 ± 1.4	5.7 ± 1.3	0.011*
Aorta vessel wall thickness (ml)	0.23 ± 0.06	0.19 ± 0.05	<0.001*
Aorta vessel wall thickness/BSA	0.12 ± 0.03	0.10 ± 0.03	<0.001*
Aorta lumen area (cm^2)	3.71 ± 0.65	3.29 ± 0.63	0.039*
Aorta lumen area / BSA (cm^2/kg)	1.95 ± 0.31	1.74 ± 0.36	0.095
Carotid vessel wall thickness (ml)	0.07 ± 0.02	0.06 ± 0.01	0.025*
Carotid vessel wall thickness/BSA	0.04 ± 0.01	0.03 ± 0.01	0.014*

BMI: body mass index; BSA: body surface area; Cholesterol/HDL ratio: cholesterol to high density lipid protein. The mean VWT is represented by cross-sectional vessel wall area × slice thickness averaged over all included slices and is indexed for BSA and expressed in ml. Data are expressed as means ± sd. * p-value < 0.05.

between age and PWV was not significantly different between patients and volunteers as the slope of the regression was not significantly different between patients and controls (p = 0.527). However, the intercept of the association between age and PWV was significantly different among patients and healthy adult volunteers (p < 0.001), indicating the significantly higher PWV in hypertensive patients as compared to healthy volunteers regardless of age. The association between age and PWV for patients and controls separately, is shown in Figure 1a.

Aortic VWT was also significantly associated with age in patients and in healthy adult subjects. Pearson r = 0.80 in hypertensive patients and r = 0.90 in controls, respectively. The association between age and aortic VWT was not significantly different between patients and controls (difference in slope: p = 0.440), but a significant difference in the intercept (difference in intercept: p < 0.001) between patients and healthy adult subjects was found, indicating the increased aortic VWT in hypertensive patients (p < 0.001) as compared to healthy adult subjects (Figure 2b).

Carotid VWT was also significantly associated with age in patients and in healthy adult subjects with r = 0.58 in hypertensive patients and r = 0.53 in controls. Again, no significant difference in the association between age and carotid VWT was found between patients and controls (difference in slope between patients and volunteers: p = 0.789). However a significant difference in intercept between patients and healthy adult subjects was found

Table 2. Associations between age, aortic PWV, aorta and carotid wall thickness in patients with hypertension versus healthy volunteers

		Slope ± se	*p-value*	*Intercept ± se*	*p-value*	*Pearson (r)*
	Hypertension	0.08 ± 0.02		3.42 ± 0.96		0.74
PWV versus age	(n=15)	0.002*		0.003*		
			0.527		<0.001*	
	Volunteers	0.06 ± 0.02		2.69 ± 0.90		0.70
	(n=15)	0.004*		0.010*		
	Hypertension	0.001 ± 0.001		0.055 ± 0.016		0.80
Aortic VWT/BSA versus age	(n=15)	<0.001*		0.005*		
			0.440		<0.001*	
	Volunteers	0.002 ± 0.001		0.018 ± 0.012		0.90
	(n=15)	<0.001		0.145		
	Hypertension	0.001 ± 0.001		0.021 ± 0.008		0.58
Carotid VWT/BSA versus age	(n=15)	0.042*		0.011*		
			0.789		0.017*	
	Volunteers	0.001 ± 0.001		0.017 ± 0.005		0.53
	(n=15)	0.009*		0.001*		
	Hypertension	0.013 ± 0.003		0.034 ± 0.022		0.76
Aortic VWT/BSA versus PWV	(n=15)	0.002*		0.181		
			0.949		0.341	
	Volunteers	0.012 ± 0.005		0.029 ± 0.028		0.63
	(n=15)	0.023*		0.373		
	Hypertension	0.004 ± 0.002		0.014 ± 0.011		0.50
Carotid VWT/BSA versus PWV	(n=15)	0.037*		0.095		
			0.520		0.350	
	Volunteers	0.002 ± 0.001		0.020 ± 0.008		0.40
	(n=15)	0.130		0.009*		
	Hypertension	0.269 ± 0.081		0.006 ± 0.010		0.60
Carotid VWT/BSA versus aortic VWT/BSA	(n=15)	0.005*		0.049*		
			0.320		0.620	
	Volunteers	0.172 ± 0.054		0.016 ± 0.006		0.57
	(n=15)	0.007*		0.616		

se: standard error; PWV: pulse wave velocity; VWT: vessel wall thickness; The mean VWT is represented by cross-sectional vessel wall area × slice thickness averaged over all included slices and is indexed for body surface area (BSA) and expressed in ml. * p-value < 0.05.

(difference in intercept: p = 0.017), indicating the increased carotid VWT in patients as compared to healthy adult subjects (Figure 2c).

PWV was significantly associated with VWT in the aorta in both patients (r = 0.76) and healthy adult subjects (r = 0.63). However, the association was not significantly different between patients and healthy adult subjects with (no significant difference in slope, p = 0.949 nor in intercept p = 0.341) between patients and controls. From Figure 2d, it can be observed

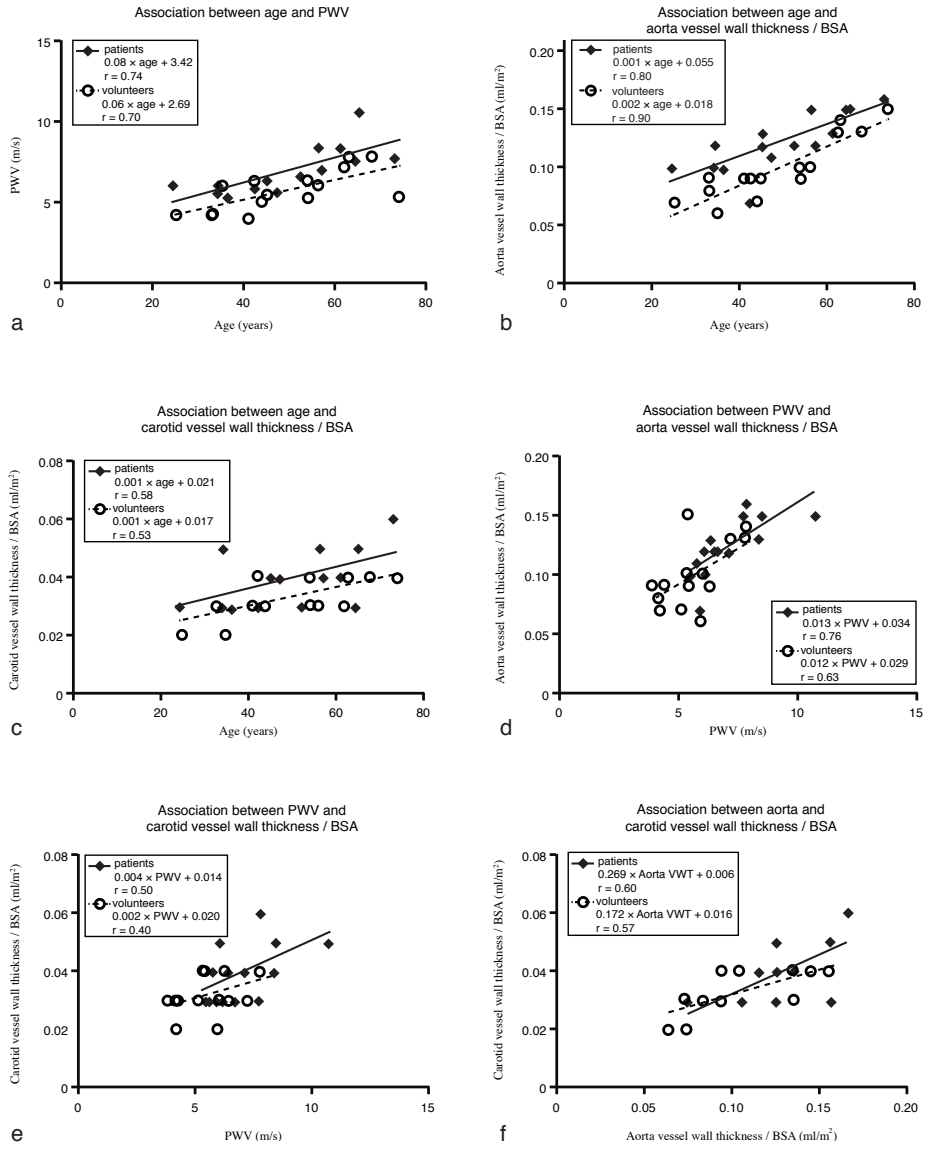

Figure 2. Associations between age, aortic VWT, carotid VWT and aortic PWV in hypertension and healthy volunteers.
Association between age and aortic pulse wave velocity (PWV) (a), aortic VWT indexed for body surface area (BSA) (b) and carotid VWT indexed for body surface area (BSA) (c), respectively, in hypertensive patients and age- and sex-matched healthy volunteers. Association between aortic PWV and aortic VWT indexed for body surface area (BSA) (d) and carotid VWT indexed for body surface area (BSA) (e), respectively, in hypertensive patients and age- and sex-matched healthy volunteers. Association between aortic VWT indexed for body surface area (BSA) and carotid VWT indexed for body surface area (BSA) (f) in hypertensive patients and age- and sex-matched healthy volunteers.

that regression lines are approximately similar between patients and healthy adult subjects. From the distribution and range of the data in this graph it is obvious that patients have increased PWV-values and aortic VWT as compared to healthy adult subjects.

Furthermore, PWV was significantly associated with VWT in the carotid artery in patients (r = 0.50), but not in controls (r = 0.40). However, the association was not significantly different between patients and healthy adult subjects with comparable slopes (p = 0.520) and no significant difference in intercept (0.350). From the distribution and range of the data in Figure 2e, it can be observed that both PWV and carotid VWT are increased in patients as compared to healthy adult subjects.

Finally, both in patients and in controls, aortic VWT was significantly associated with carotid VWT (r 0.60 and 0.57, respectively). This association between aortic and carotid VWT was not significantly different between patients and controls with no significant difference in the slope (p = 0.320) nor in the intercept (p = 0.620) between patients and healthy adult subjects. This can also be observed in Figure 2f. Furthermore, the distribution and range of the data in Figure 2f shows that patients have increased aorta and carotid VWT as compared to healthy adult subjects.

Discussion

The main observations from this study are:

First, aortic PWV and VWT in the aorta and carotid artery are increased in patients with hypertension as compared to healthy adult subjects. Second, aortic PWV is significantly and positively associated with aortic VWT in both hypertensive patients and healthy adult subjects. Third, aortic PWV and aortic VWT are equally positively associated with carotid VWT in both hypertensive patients and healthy adult subjects. Thus, an increase in aortic stiffness relates to an increase in VWT in both the aorta and carotid arteries, similarly in hypertensive patients and healthy adult subjects. Finally, all variables are age-related similarly in both investigated sub-groups.

It is well known that aortic PWV and VWT in the aorta and carotid arteries are increased in patients with hypertension (3,12,18-20). Hypertension is a systemic disease that causes structural changes in the arterial vessel wall, due to fracture and fragmentation of the elastin fibers, with consequent increase in VWT and decrease in vessel wall compliance or elasticity (20). According to the Moens-Korteweg equation, PWV is dependent on the elastic properties, aortic diameters and thickness of the vessel wall (21). However, in the current study, aortic diameter (as reflected in aortic lumen area) did not differ between hypertensive patients and healthy adult subjects. This finding may indicate that changes in aortic PWV and aortic wall thickness are earlier manifestations of aortic vessel wall alterations than aortic lumen dilatation.

In the current study, MR-assessed increased aortic PWV was associated with increased aortic VWT both in hypertensive patients and in controls. To the best of our knowledge, direct association between aortic PWV and aortic VWT has not been reported before. Furthermore,

aortic PWV is associated with carotid VWT. Several studies have described the association between arterial stiffness and increased carotid intima-media thickness (6-8). However, as these studies used ultrasound assessment, no comprehensive evaluation of aortic vessel wall alterations could be performed and consequently, association between aortic PWV and aortic VWT could not be reported. In contrast to ultrasound techniques, MRI is a well-suited and validated modality for accurate assessment of aortic PWV as well as aorta and carotid VWT and therefore direct evaluation of the associations between aortic PWV and VWT with carotid VWT is feasible (9,10,22).

Although hypertension is regarded as a systemic disease, it has been suggested that the development of arterial wall alterations starts in the aorta first and then progresses to the more peripheral arteries, including the carotid arteries (5,23,24). This study may provide evidence for this hypothesis as the association between aortic PWV and aortic VWT was higher than the association between aortic PWV and carotid VWT. Assessment of aortic PWV may have clinical relevance in hypertensive patients. Previously, an MRI-study has demonstrated in asymptomatic hypertensive patients that increased aortic PWV independently predicts cardiac and cerebral end-organ disease (13). Similarly, the current study shows that MRI can assess early systemic vessel wall alterations. Such information may be valuable for risk stratification and patient management.

Our study has some limitations. First, it involves a cross-sectional study design. Follow-up studies in patients with other diseases than hypertension need to be performed to further elucidate the associations between aortic PWV and VWT in the aorta and carotid arteries in other patient groups. Second, because of medical ethical reasons, all patients were taking antihypertensive medication at time of MRI, which could have influenced aortic and carotid measurements in patients with hypertension. However, this medication also has a beneficial effect on arterial stiffness, therefore the differences in PWV would only increase if patients were not on medication. Third, we performed vessel wall measurements at 3T to improve accuracy as compared to lower field strengths. Flow measurements for PWV assessment can however equally well be performed at 1.5 and 3T. Fourth, in this study, sampling of the aortic VWT was limited to a 2 cm segment of the proximal descending aorta and sampling of the carotid VWT was limited to a 1.6 cm of the left common carotid artery only. The sample sites were well standardized for comparison purposes. Sampling at longer segments or other vascular trajectories is possible at the penalty of longer scan time. In the future sampling other vascular territories may add more information on the systemic nature of the disease.

In conclusion, using standardized and validated MRI protocols, we have demonstrated that functional and morphological alterations, namely aortic PWV and aortic VWT are significantly associated. This also applies to aortic PWV and carotid VWT - albeit to a lesser extent. These findings also indicate the systemic nature of early vessel wall thickening associated with hypertension, potentially allowing improved risk stratification of hypertensive vascular disease.

References

1. Chobanian AV, Bakris GL, Black HR, et al. Seventh report of the Joint National Committee on Prevention, Detection, Evaluation, and Treatment of High Blood Pressure. Hypertension 2003;42:1206-1252.
2. Mancia G, De Backer G, Dominiczak A, et al. 2007 Guidelines for the Management of Arterial Hypertension: The Task Force for the Management of Arterial Hypertension of the European Society of Hypertension (ESH) and of the European Society of Cardiology (ESC). J Hypertens 2007;25:1105-1187.
3. Cecelja M, Chowienczyk P. Dissociation of aortic pulse wave velocity with risk factors for cardiovascular disease other than hypertension: a systematic review. Hypertension 2009;54:1328-1336.
4. Cecelja M, Chowienczyk P. Arterial stiffening: cause and prevention. Hypertension 2010;56:29-30.
5. Paini A, Boutouyrie P, Calvet D, Tropeano AI, Laloux B, Laurent S. Carotid and aortic stiffness: determinants of discrepancies. Hypertension 2006;47:371-376.
6. van Popele NM, Grobbee DE, Bots ML, et al. Association between arterial stiffness and atherosclerosis: the Rotterdam Study. Stroke 2001;32:454-460.
7. Zureik M, Temmar M, Adamopoulos C, et al. Carotid plaques, but not common carotid intima-media thickness, are independently associated with aortic stiffness. J Hypertens 2002;20:85-93.
8. Tartiere JM, Logeart D, Safar ME, Cohen-Solal A. Interaction between pulse wave velocity, augmentation index, pulse pressure and left ventricular function in chronic heart failure. J Hum Hypertens 2006;20:213-219.
9. Alizadeh DR, Doornbos J, Tamsma JT, et al. Assessment of the carotid artery by MRI at 3T: a study on reproducibility. J Magn Reson Imaging 2007;25:1035-1043.
10. Roes SD, Westenberg JJ, Doornbos J, et al. Aortic vessel wall magnetic resonance imaging at 3.0 Tesla: a reproducibility study of respiratory navigator gated free-breathing 3D black blood magnetic resonance imaging. Magn Reson Med 2009;61:35-44.
11. Grotenhuis HB, Westenberg JJ, Steendijk P, et al. Validation and reproducibility of aortic pulse wave velocity as assessed with velocity-encoded MRI. J Magn Reson Imaging 2009;30:521-526.
12. Malayeri AA, Natori S, Bahrami H, et al. Relation of aortic wall thickness and distensibility to cardiovascular risk factors (from the Multi-Ethnic Study of Atherosclerosis [MESA]). Am J Cardiol 2008;102:491-496.
13. Brandts A, van Elderen SG, Westenberg JJ, et al. Association of aortic arch pulse wave velocity with left ventricular mass and lacunar brain infarcts in hypertensive patients: assessment with MR imaging. Radiology 2009;253:681-688.
14. van der Geest RJ, de Roos A, van der Wall EE, Reiber JH. Quantitative analysis of cardiovascular MR images. Int J Card Imaging 1997;13:247-258.
15. Edelman RR, Chien D, Kim D. Fast selective black blood MR imaging. Radiology 1991;18:655-660.
16. Adame IM, van der Geest RJ, Bluemke DA, Lima JA, Reiber JH, Lelieveldt BP. Automatic vessel wall contour detection and quantification of wall thickness in in-vivo MR images of the human aorta. J Magn Reson Imaging 2006;24:595-602.
17. Adame IM, van der Geest RJ, Wasserman BA, Mohamed MA, Reiber JH, Lelieveldt BP. Automatic segmentation and plaque characterization in atherosclerotic carotid artery MR images. MAGMA 2004;16:227-234.
18. Laurent S, Boutouyrie P, Asmar R, et al. Aortic stiffness is an independent predictor of all-cause and cardiovascular mortality in hypertensive patients. Hypertension 2001;37:1236-1241.

19. Safar H, Mourad JJ, Safar M, Blacher J. Aortic pulse wave velocity, an independent marker of cardiovascular risk. Arch Mal Coeur Vaiss 2002 ;95:1215-1218.
20. Benetos A, Laurent S, Hoeks AP, Boutouyrie PH, Safar ME. Arterial alterations with aging and high blood pressure. A noninvasive study of carotid and femoral arteries. Arterioscler Thromb 1993;13:90-97.
21. Mitchell GF, Conlin PR, Dunlap ME, et al. Aortic diameter, wall stiffness, and wave reflection in systolic hypertension. Hypertension 2008:51;105-111.
22. Maroules CD, McColl R, Khera A, Peshock RM. Assessment and reproducibility of aortic atherosclerosis magnetic resonance imaging: impact of 3-Tesla field strength and parallel imaging. Invest Radiol 2008;43:656-662.
23. Lakatta EG, Levy D. Arterial and cardiac aging: major shareholders in cardiovascular disease enterprises: Part I: aging arteries: a "set up" for vascular disease. Circulation 2003;107:139-146.
24. Lakatta EG, Levy D. Arterial and cardiac aging: major shareholders in cardiovascular disease enterprises: Part II: the aging heart in health: links to heart disease. Circulation 2003;107:346-354.